Fermi National Accelerator Laboratory

FN-375
7180.605

CONSTRUCTION AND OPERATION OF A LARGE RING-IMAGING CERENKOV DETECTOR*

H. Glass, M. Adams, A. Bastin, G. Coutrakon, D. Jaffe,
J. Kirz, and R. McCarthy
State University of New York at Stony Brook, Stony Brook, New York 11794 USA

and

J. R. Hubbard, Ph. Mangeot, J. Mullie, A. Peisert, and J. Tichit
CEN Saclay, F91190 Gif-sur-Yvette, France

and

R. Bouclier, G. Charpak, J. C. Santiard, and F. Sauli
CERN, EP Division, 1211 Geneva 23, Switzerland

and

J. Crittenden, Y. Hsiung, and D. Kaplan
Columbia University, Nevis Labs, Box 137, Irvington, New York 10533 USA

and

C. Brown, S. Childress, D. Finley, A. Ito, A. Jonckheere, H. Jostlein,
L. Lederman, R. Orava, S. Smith, K. Sugano, and K. Ueno
Fermi National Accelerator Laboratory, Batavia, Illinois 60510 USA

and

A. Maki
KEK, Tsukuba-gun, Ibaraki-ken, 305 Japan

and

Y. Hemmi, K. Miyake, T. Nakamura, N. Sasao, and Y. Sakai
Kyoto University, Kyoto 606 Japan

and

R. Gray, R. Plaag, J. Rothberg, J. Rutherfoord, and K. Young
University of Washington, Seattle, Washington 98195 USA

December 1982

*Talk presented at the IEEE Nuclear Science Symposium, Washington, D. C., October 20-22, 1982.

Operated by Universities Research Association Inc. under contract with the United States Department of Energy

CONSTRUCTION AND OPERATION OF A LARGE RING-IMAGING CERENKOV DETECTOR

H. Glass, M. Adams, A. Bastin, G. Coutrakon, D. Jaffe, J. Kirz and R. McCarthy

SUNY at Stony Brook, Stony Brook, NY 11794

J.R. Hubbard, Ph. Mangeot, J. Mullie, A. Peisert and J. Tichit

CEN Saclay, F91190 Gif-sur-Yvette, France

R. Bouclier, G. Charpak, J.C. Santiard and F. Sauli

CERN, EP Division, 1211 Geneve 23, Switzerland

J. Crittenden, Y. Hsiung and D. Kaplan

Columbia University, Nevis Labs, Box 137, Irvington, NY 10533

C. Brown, S. Childress, D. Finley, A. Ito, A. Jonckheere, H. Jostlein, L. Lederman, R. Orava, S. Smith, K. Sugano and K. Ueno

FNAL, Box 500, Batavia, IL 60510

A. Maki

KEK, Tsukuba-gun, Ibaraki-ken, 305 Japan

Y. Hemmi, K. Miyake, T. Nakamura, N. Sasao and Y. Sakai

Kyoto University, Kyoto, 606 Japan

R. Gray, R. Plaag, J. Rothberg, J. Rutherfoord and K. Young

University of Washington, Seattle, WA 98195

Summary

We have constructed a large-aperture ring-imaging Cerenkov counter, intended to identify high momentum hadrons in a high p_t experiment at Fermilab (E605). To date we have performed a preliminary analysis on a small subset of our data, taken during the initial operation of our counter (April-June 1982). We have obtained π/K separation with good efficiency from about 60 GeV/c to 120 GeV/c in momentum under high luminosity conditions ($\sim 5 \times 10^9$ protons/second on target). Approximately 84% of all single-track events having at least one detected photon have been unambiguously identified. Cerenkov photons were detected by a multi-step avalanche chamber via the photoionization of triethylamine (TEA) vapor, and a mean number of 2.8 photons per event was detected for the highest velocity particles. Improvements in photon reconstruction are expected, especially as we refine our tracking procedures.

Experimental configuration. Figure 1 is a diagram of Fermilab Experiment 605. Our Cerenkov counter is separated from the target by two spectrometer magnets (total kick ~6 GeV for this data) which help reduce particle fluxes at our counter. We accept particles over a wide angular range (±60 mrad vertically). Hadronic trajectories were selected using our calorimeter system and tracked by our chamber system.

Cerenkov Counter Description

Radiator vessel

The design of our Cerenkov counter is based upon a successful prototype[1]. We used pure helium as the radiator gas in order to limit chromatic dispersion. The radiator vessel is a thin-walled (3/32 inch) aluminum (6061-T6) box. All permanent joints in this structure were welded, taking care to avoid pinholes. Non-permanent joints (at the detector and monitoring ports) were sealed with viton O-rings. Structural strength was provided by aluminum channels and I-beams exterior to the vessel. The side walls were allowed to flex under pressure changes without cracking any welds. The vessel is 15.2 m long and 3.1 x 2.8 m^2 in cross section at its widest point (near the detectors). The length is sufficient to obtain about 6 detected photons from one particle[1], assuming 100% He transmission, and the cross section was chosen to contain all trajectories of experimental interest.

The vessel has two detector ports, one on each side. For this initial run, only one port was used. The ports are located outside the experimental aperture, and so only Cerenkov photons are seen by the detectors.

Our paramount concern in constructing the Cerenkov vessel was that the helium radiator gas should not be-

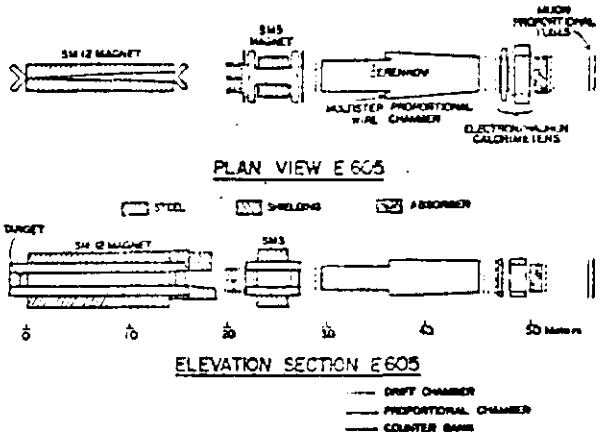

Fig. 1. Experiment E-605.

come contaminated. Since purity better than 1 ppm is required against some contaminants (oxygen), care was taken to eliminate all materials from the vessel other than aluminum, steel, viton, glass, MgF_2, and CaF_2. The vessel was cleaned with freon, flushed with nitrogen gas and baked at 100 C for 48 hours before filling with pure helium from liquid boiloff.

The radiator gas was maintained at room temperature and slightly above atmospheric pressure. For typical running conditions, the mean index of refraction was $n^2-1 = 72.0 \times 10^{-6}$, giving a threshold γ_t = 118. This translated into threshold momenta of 16 GeV/c for π's, 58 GeV/c for K's, and 110 GeV/c for p's.

Gas purification system

The photon transmission of the He gas was maintained by recirculation through a purification system. As the gas enters the purifier it is mixed with a small amount of hydrogen and put through a Deoxo catalyzer (Engelhard Systems, N.J.). The gas then passes through a dryer and a liquid nitrogen cold trap, which extract and freeze out gas impurities. Gas purity was monitored using a UV light source[1], and the gas transmission was measured to be about 80%, a value somewhat lower than anticipated. Flow rate through the purifier was approximately two volume changes per day.

Mirrors

The full mirror assembly consists of a 4 x 4 array of mirror segments, each a 25 x 26 in^2 rectangle. For this initial run, only 8 of the mirror segments were available. These segments were placed in the two central columns of our array, subtending an area 52 x 100 in^2 (half the aperture). Both mirror columns were focussed onto the right (as seen by an incident proton) detector port.

We used the largest segments available consistent with good reflectivity at 1500 angstroms. Each segment[2] was ground from a 7/8 inch thick blank of annealed plate glass to a spherical radius of 16.00 ±0.02 m. The surface was polished to an rms roughness less than 30 angstroms. The figure accuracy of the spherical surface was better than 20 urad (error in the normal) over any 18 cm diameter circle. The spherical surfaces were coated with aluminum and MgF_2 to attain a reflectivity of 75% at 1500 angstroms.

The mirrors were hung from above using piano wire. Adjustments in mirror orientation were made from behind, relative to a light aluminum grid. The mass of this grid is mostly located in the mirror gaps in an attempt to keep the mass distribution uniform across the mirror surface. Each mirror segment is held in its own aluminum frame, cushioned by viton.

The mirrors were aligned visually to ±1 cm accuracy in image position on the detector plane. Our system is self-calibrating using particle tracks with three or more photons. Each mirror was independently aligned so that ring images from adjacent mirrors were non-overlapping. This is done to minimize confusion in point reconstruction. Mirror alignment angles were chosen so as to minimize the necessary detector area required to see trajectories over the whole aperture.

Calcium fluoride window

The window assembly separating the radiator gas from the detector gas was a 4 x 8 mosaic of CaF_2 crystals, each 10 x 10 cm^2 in area and 4 mm thick. Each crystal was glued to a heavy brass frame, whose thermal expansion properties were similar to those of the crystals. The frame was maintained at the same voltage as the first grid of the detector to minimize electrostatic instabilities. The transmission of the crystals was typically 70%.

Photon detector

The photon detector was a multi-step proportional chamber with a 40 x 80 cm^2 active area. Figure 2 shows schematically the CaF_2 window, the conversion, preamplification, and transfer gaps (made of stainless steel grids), the proprtional wire chamber, and an external double mylar window. This structure was similar to that of the smaller prototype detector described previously[1,3]

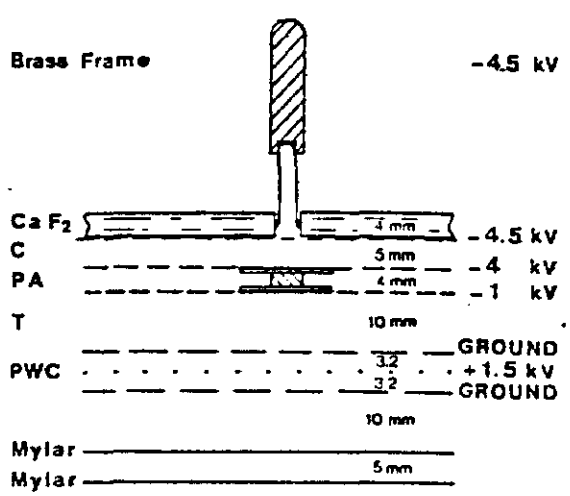

Fig. 2. The multi-step avalanche chamber, showing spacing between planes and typical operating voltages.

Spacers were necessary in the PA gap to maintain uniform gap thickness and thus avoid huge increases in gain in the center of the chamber due to electrostatic attraction of the two grids[3,4]. Three carefully machined fiberglass spacers were used, with mylar guard rings. Gain variations were less than 50%.

The proportional chamber anode plane consisted of 192 vertical 20-micron diameter wires spaced every 2 mm. The cathode wires were oriented at ±45 degrees with respect to the anodes. Each cathode contained 2 x 384 50-micron diameter wires spaced every 1 mm. The chamber was operated with a He(97%)/TEA(3%) gas mixture at a gain of about 10^7.

Readout system

The anode and cathode wires were read out every 2 mm into LeCroy 2280-series 12-bit ADC's. The LeCroy ADC system is controlled by a processor module which automatically performs pedestal subtraction and data compression. The processor data was read out via CAMAC into an on-line PDP 11/45 computer. On-line monitoring of the detector was performed via the Fermilab MULTI software package.

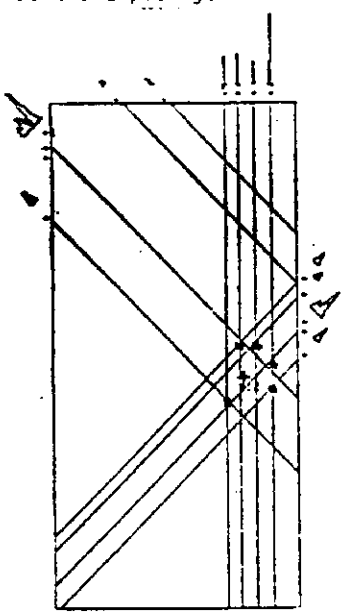

Fig. 3. An off-line display of a 5-photon K event. Cathode pulses are seen angled in the left and right margins, and anode pulses at the top. The reconstructed photon positions are indicated by *'s, and the predicted ring center by +.

Particle Identification Procedure

Pulse height information from the ADC's is used to measure the coordinates of each Cerenkov photon. Cathode pulses are spread over 5-6 ADC channels, and a center-of-gravity method is used to find the pulse center. Anode pulses generally cover a single wire. The point reconstruction algorithm searches for cathode-cathode-anode triplets, rejecting ghost triplets by requiring approximately equal amplitudes in all three planes.

The particle track is defined by two sets of drift chambers on either end of the Cerenkov vessel (fig. 1), and the momentum is calculated from the particle trajectory. We calculated 3 radii from the momentum, one for each particle type hypothesis, π, K, or p. Then, for each mirror capable of intercepting and reflecting photons from the particle, a ring center is calculated on the detector plane. This is done by treating the particle trajectory itself as if it were a photon: its path is traced to the mirror surface, then reflected onto the detector plane, where it defines the ring center. We then measure the distance between each photon candidate point and each calculated ring center, and try to find a set of radii consistent with one of our particle hypotheses.

Effects of Aberrations

The asymmetric geometry of our current setup introduces various aberrations. One effect is the distortion of the ring image from a circle to an approximate elliptical shape. The amount of distortion varies from mirror to mirror, and depends upon the photon trajectory, but can be calculated for each event, provided the particle track is known. The difference between major and minor axes is no worse than 1.4%, and can be corrected by the photon reconstruction program.

Another problem arises from the long radiator length: photons emitted at various points along a particle's trajectory do not come to a well-defined focus. The best that can be done is to place the detector at the circle of least confusion[5], where we obtain the optimum average focus. The ring images are also astigmatic: they are out of focus at points near the major and minor axes of the ellipse, and in focus at points in between.

For the set of mirrors on the same side of the apparatus as the photon detector, the astigmatism is very small and produces a typical uncertainty in radius of ±0.07% rms. The mirrors on the away side generate a larger astigmatism, and their ring images have uncertainties in radii of typically ±0.37% rms.

When the second detector and the full complement of 16 mirrors becomes available, a more symmetrical arrangement of mirrors and detectors will result in reducing the uncertainty due to astigmatism to ±0.07% for all mirrors. Even so, the astigmatism in the current run is tolerable with respect to particle identification.

Chromatic dispersion. Chromatic dispersion arises from the dependence of the helium index of refraction upon photon energy, and generates an rms uncertainty of ±0.7% in the radius. This effect can be reduced by adding about 10% CH_4 to the chamber gas, which absorbs higher energy photons[1,3].

Pressure and temperature effects. The index of refraction also depends upon pressure and temperature as $n^2-1 = p/T$. The temperature at various points within the Cerenkov vessel were measured by thermocouples. We observed a non-uniformity in temperature within the vessel. The observed rms uncertainty in temperature was ±0.9 K, causing an uncertainty in ring radius of ±0.15%. While both pressure and temperature fluctuated over the course of a run, the ratio p/T tended to remain roughly constant, and the drift in radius over the course of a run of several hours duration was on the order of 0.03%.

The sum in quadrature of all the above effects gives an uncertainty of ±0.78% in radius. For a pion having a radius of 68.0 mm, this is an uncertainty of ±0.53 mm.

Other factors. The two other major factors influencing radius resolution are the uncertainties in

calculating the ring center due to tracking uncertainties (involving drift chamber resolution and surveying errors), and the inherent resolution of the multi-step chamber itself. Identification of one- and two-photon events is obviously crucially dependent upon the careful measurement of the ring center, whereas three- or more-photon events have actually been used to correct our survey data, in particular the mirror alignment angles.

Preliminary Analysis Results

The track reconstruction procedures for this experiment are still in a developmental stage. Hence, tracking uncertainties completely dominate our errors at this time, and all results stated below are preliminary and are expected to improve with improvements in track reconstruction efficiency.

Number of Photons

The mean number of photons produced by a particle is proportional to $\sin^2 \theta_c$, where θ_c is the Cerenkov angle. For the detector to be effective, the mean number of detected photons must be high enough so that the probability of an event generating zero photons is small; on the other hand, the mean number of detected photons must be low enough so that reconstruction efficiency does not become crippled by inability to separate many overlapping coordinates. In our application, about 5 or 6 photons per event is the optimal situation, and we have designed our counter with this number of photons as a goal.

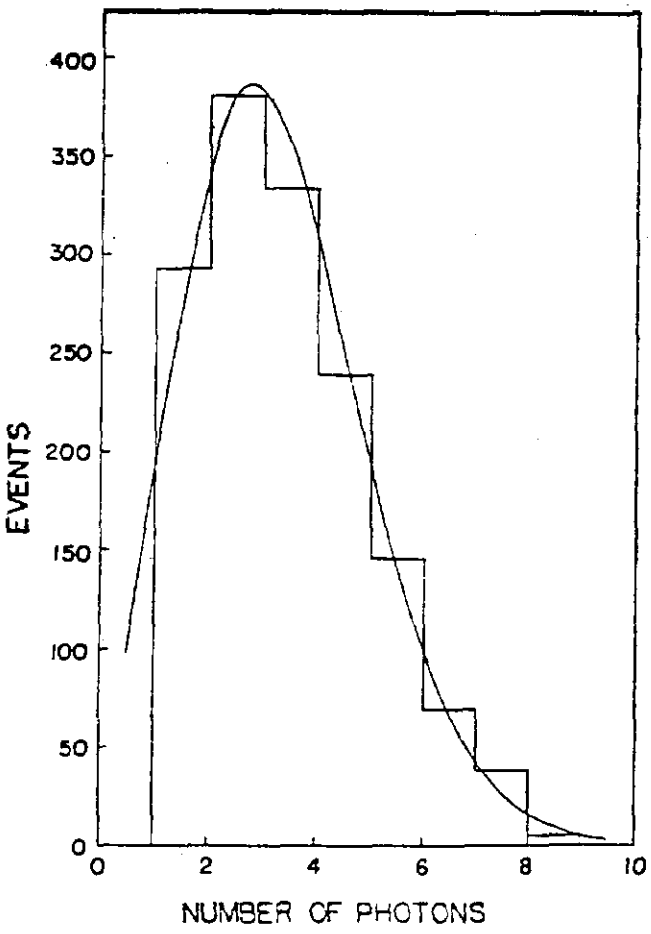

Fig. 4. Distribution of the number of photons for π's. A Poisson distribution with a mean of 2.8 is superimposed. For this fit, χ^2 = 11.0 for 8 degrees of freedom.

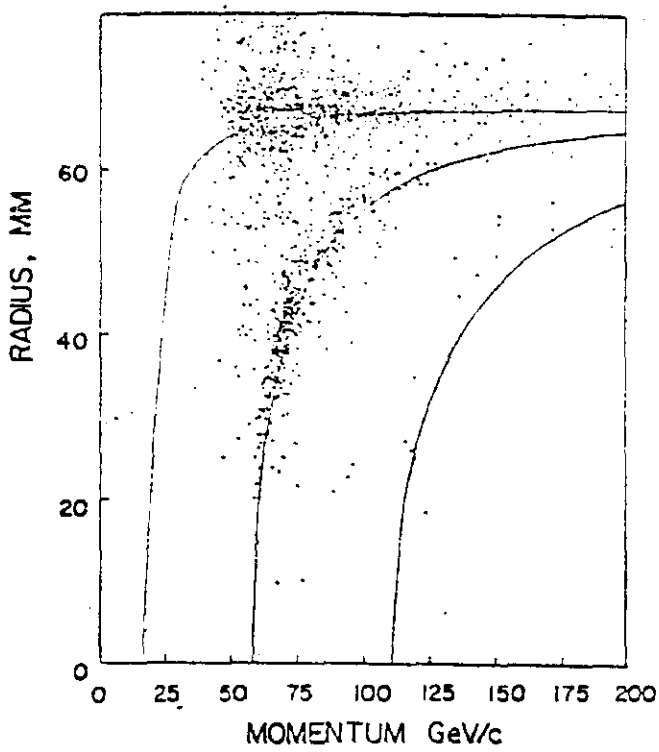

Fig. 5. Scatter plot of radius vs momentum for events having at least one reconstructed photon. Curves showing the expected radii for π,K, and p are superimposed.

We have measured the mean number of photons from identified pions, all of which have radii near the maximum, to be about 2.8 per event. The number of photons fits a Poisson distribution rather well (fig. 4), and extrapolation gives the result that about 6% of the pions are lost because of zero photons. The reasons for the lower than expected number of photons is under study. We are aware that the relatively poor helium transmission is a factor.

π-K Separation

Kaons have been identified with a mean number of photons equal to 1.8 per event. Looking at a scatter plot of radius vs. momentum (fig. 5), we see a clear separation between the π-K bands out to 120 GeV/c. A few proton events are also observed. The width of the π peak as seen in the radius distribution of figure 6 is about 4 mm FWHM. Reduction of this width, which will become possible with improvements in tracking and surveying, will enable π-K separation at higher momenta.

Particle Identification Results

Table I summarizes the particle identification results over a variety of runs, including data from Be, Cu, and W targets. These events required a hadron calorimeter trigger threshold energy of about 50 GeV. We have so far analyzed only single-track events; we plan to reconstruct multi-track events at a later stage. The major problem of multi-track events is the problem of disentangling overlapping ring images from different particles.

For the single hadron sample, we have unambiguously identified 83.6% of the events having one or more photons. Both positive and negative hadrons have been identified.

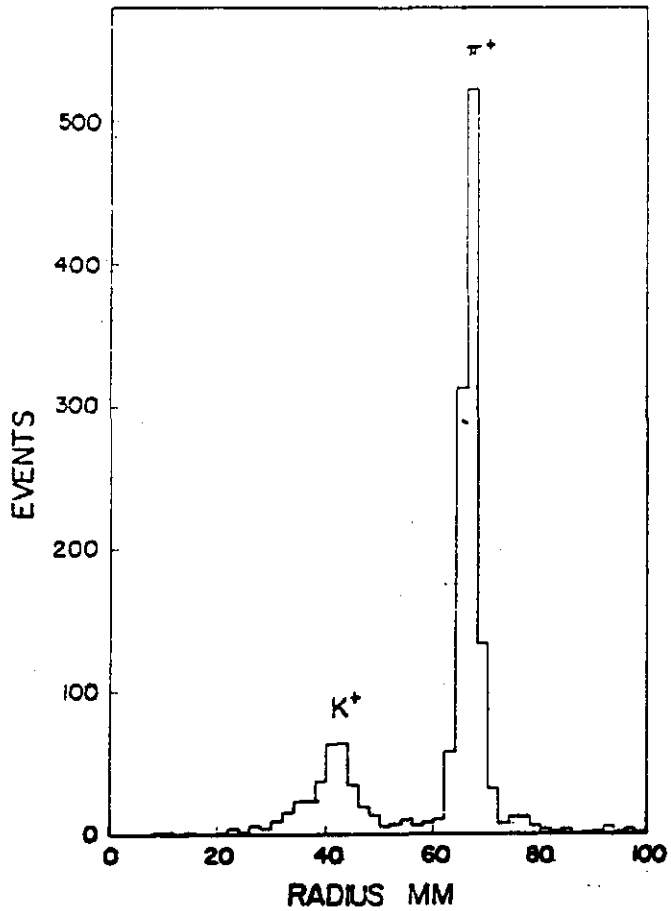

Fig. 6. Radius distribution for events in the momentum band 60<p<80 GeV/c.

Zero-photon events. The large number of zero-photon events is found to be consistent with the expectation of a large number of below-threshold protons. An estimate of the contribution of π's and K's to the zero-photon sample is calculated as a function of momentum, based on the observed mean number of photons. We find the π^+/K^+ ratio, including the estimated contribution for events lost due to zero photons, is roughly constant with total momentum and is approximately equal to 2. After subtracting the π-K contribution to the zero-photon sample, we find the ratio π^+/p to be approximately 1.2 and constant over a momentum range 60-100 GeV/c. Both observed ratios are in rough agreement with measurements by a previous experiment[6]. We find that from about 75 GeV/c up to proton threshold at 110 GeV/c, zero-photon events can be interpreted as protons with 80% or better confidence.

Total number of events in sample = 13642

Particles identified by at least one photon:

π^+ = 5184	π^- = 536	total π = 5720
K^+ = 1307	K^- = 38	total K = 1345
p = 25	$\bar{p}$ = 1	total $p,\bar{p}$ = 26

Ambiguous events = 1515

Zero-photon events = 5165

Table I. Summary of preliminary particle identification results for single-track hadron events.

Acknowledgments

The authors wish to thank the staffs of Stony Brook, Saclay, CERN, and Fermilab for their technical expertise. This work was supported in part by grants from the National Science Foundation and the Department of Energy.

References

1. G. Coutrakon et. al., IEEE Transactions on Nuclear Science NS-29 (1982) 323.
2. purchased from Muffoletto Optical Company, 6100 Everall Avenue, Baltimore, MD 21206.
3. R. Bouclier et. al., CERN-EP/82-83, submitted to N.I.M.
4. J.R. Hubbard et. al., N.I.M. 176 (1980) 293.
5. see, for example, F. Jenkins and H. White, Fundamentals of Optics, McGraw-Hill (1957).
6. H. Jostlein et. al., Phy. Rev. D20 (1979) 53.